Validation of Asphalt Binder and Mixture Tests That Measure Rutting Susceptibility

FHWA-RD-99-204

NOVEMBER 2000

U.S. Department of Transportation
Federal Highway Administration

Research, Development, and Technology
Turner-Fairbank Highway Research Center
6300 Georgetown Pike
McLean, VA 22101-2296

FOREWORD

This report documents a Federal Highway Administration (FHWA) research study that was performed to assist the highway community in validating Superpave tests and specifications being used to grade asphalt binders according to their relative rutting resistances. Superpave and other asphalt mixture tests for rutting were also evaluated.

To accomplish the objective, twelve full-scale pavements were constructed at the FHWA Pavement Testing Facility in 1993. This facility is located at the Turner-Fairbank Highway Research Center in McLean, VA. The pavements were tested for rutting resistance by an Accelerated Loading Facility, which applies one-half of a rear truck axle load. The asphalt binder and mixture tests were validated using the results from these pavement tests.

This document will be of interest to people involved with Superpave and the evaluation of hot-mix asphalts for rutting performance. Recommendations are given concerning a wide range of tests. Asphalt binder and mixture tests used to measure fatigue cracking resistance were also evaluated in this project. The results will be presented in a future report

This report is being distributed on a limited basis. Copies of this report are available from the National Technical Information Service (NTIS), 5285 Port Royal Road, Springfield, Virginia 22161.

T. Paul Teng

T. Paul Teng, P.E.
Director, Office of Infrastructure
Research and Development

NOTICE

Technical Report Documentation Page

1. Report No.	2. Government Accession No.	3. Recipient's Catalog No.
FHWA-RD-99-204		

4. Title and Subtitle

VALIDATION OF ASPHALT BINDER AND MIXTURE TESTS THAT MEASURE RUTTING SUSCEPTIBILITY USING THE ACCELERATED LOADING FACILITY

5. Report Date

6. Performing Organization Code

7. Author(s)

Kevin D. Stuart, Walaa S. Mogawer, and Pedro Romero

8. Performing Organization Report No.

9. Performing Organization Name and Address

Office of Infrastructure R&D
Federal Highway Administration
6300 Georgetown Pike
McLean, VA 22101-2296

10. Work Unit No. (TRAIS)

11. Contract or Grant No.

In-House Report

12. Sponsoring Agency Name and Address

Office of Infrastructure R&D
Federal Highway Administration
6300 Georgetown Pike
McLean, VA 22101-2296

13. Type of Report and Period Covered

Interim Report
October 1993 - October 1999

14. Sponsoring Agency Code

15. Supplementary Notes

For additional information on this study, contact Kevin D. Stuart, HRDI-11, Federal Highway Administration, 6300 Georgetown Pike, McLean, VA 22101-2296

16. Abstract

The Accelerated Loading Facility (ALF) was used to validate the Superpave asphalt binder parameter for rutting, namely, G*/sin(delta), and several laboratory mixture tests that have been developed to predict or compare rutting performance. The ALF is a full-scale, pavement testing machine that applies one half of a single rear truck axle load.

The asphalt binders used in this study were AC-5, AC-10, AC-20, Novophalt, and Styrelf I-D, having Superpave high-temperature continuous Performance Grades (PG's) of 59, 65, 70, 77, and 88, respectively. This is the temperature at 2.20 kPa after rolling thin-film oven aging. A dynamic shear rheometer was used to obtain these data. All five binders were used with an aggregate gradation having a nominal maximum aggregate size of 19.0 mm. The PG 59 and 70 binders were also used with a gradation having a nominal maximum aggregate size of 37.5 mm. Pavements with these materials were tested by the ALF.

The relationship between G*/sin(delta) and ALF pavement rutting performance at temperatures ranging from 46 to 76 C was poor. However, the trend was correct for the unmodified binders, and the 2.20-kPa criterion used by the Superpave binder specification appeared to be valid. The main discrepancy was provided by the two modified binders, which were both highly resistant to rutting. The G*/sin(delta) for Styrelf was higher than for Novophalt, but the pavement with Novophalt was more resistant to rutting. This discrepancy was not resolved, although tests performed on mastics indicated that the relative rutting performances of the modified binders may have to be based on mastic properties.

The ALF, French Pavement Rutting Tester, Hamburg Wheel-Tracking Device, Georgia Loaded-Wheel Tester, an unconfined repeated load compression test, and six Superpave Shear Tester measurements ranked the five 19.0-mm mixtures the same as ALF based on the average test data. The rankings based on statistics were generally different, but they were similar to ALF. Therefore, any of these tests can be used to estimate the effects of various asphalt binders on rutting.

Four mixtures, consisting of the two gradations with the PG 59 and PG 70 binders, were used to determine the effect of increased nominal maximum aggregate size and the associated 0.85-percent decrease in optimum binder content on rutting performance. None of the laboratory mixture tests matched the ALF pavement rutting performances of the four mixtures. The tests listed above were sensitive to binder grade but not to aggregate gradation. The PURWheel was sensitive to gradation but did not distinguish the PG 59 binder from the PG 70 binder. The sensitivities of these tests to other key mixture variables need to be determined in future studies.

17. Key Words	18. Distribution Statement
APT, ALF, rutting susceptibility, Superpave, wheel-tracking devices, GTM, AAMAS, repeated load tests, SST, simple shear test, STOA, short-term oven aging, wheel track testers, DSR, large stone mixtures	No restrictions. This document is available to the public through the National Technical Information Service, Springfield, Virginia 22161.

19. Security Classif. (of this report)	20. Security Classif. (of this page)	21. No. of Pages	22. Price
Unclassified	Unclassified	348	

Form DOT F 1700.7 (8-72) Reproduction of completed page authorized

PROJECT PERSONNEL

The Turner-Fairbank Highway Research Center's Bituminous Mixtures Laboratory personnel who worked on this study were:

Mr. Kevin D. Stuart, Federal Highway Administration (FHWA)
Dr. Pedro Romero, SaLUT Inc., Beltsville, MD
Mr. Frank G. Davis, Jr., SaLUT
Mr. Scott M. Parobeck, SaLUT
Mr. Brian D. Newman, SaLUT
Dr. Walaa S. Mogawer, UMASS Dartmouth, North Dartmouth, MA
Mr. Richard P. Izzo, Texas Department of Transportation, Austin, TX

The Turner-Fairbank Highway Research Center's Pavement Binders and Analytical Chemistry Laboratory personnel who worked on this study were:

Dr. Brian H. Chollar, FHWA
Dr. Naga Shashidhar, SaLUT
Ms. Susan Needham, SaLUT
Dr. Mohammed Memon, SaLUT

Personnel in charge of operating the FHWA Accelerated Loading Facility (ALF) and collecting pavement data were:

Mr. James A. Sherwood, FHWA
Mr. Eugene Genova, Halifax (Halifax Corporation, Alexandria, VA)
Dr. Xicheng Qi, Halifax (Currently with SaLUT)
Mr. Mario Tinio, Halifax (Currently with SaLUT)
Mr. Dennis Lim, Halifax (Currently with SaLUT)

Dr. Ramon F. Bonaquist, formerly with the FHWA and currently the president of Advanced Asphalt Technologies, Sterling, VA, was in charge of the experimental design for the pavements and pavement construction. Dr. Bonaquist also directed the operation of the ALF at the time of pavement construction. The experimental design was developed in cooperation with the Strategic Highway Research Program (SHRP). The SHRP staff were Dr. Edward T. Harrigan and Dr. Rita B. Leahy, along with Professor Carl L. Monismith, University of California at Berkeley, and Mr. James S. Moulthrop, Sr. Dr. Harrigan is currently a senior staff member with the National Cooperative Highway Research Program, Washington, D.C.; Dr. Leahy is with Furgo-BRE, Austin TX, and Mr. Moulthrop is with Koch Materials, Austin, TX. The FHWA Eastern Federal Lands Highway Division, Sterling, VA, administered the construction contract. Frank Fee, formerly with Koch Materials and currently with CITGO Asphalt Refining Company, Moylan, PA, assisted the FHWA in obtaining the asphalt binders. Dr. Ernest Bastian, FHWA, Dr. Chris Williams, FHWA, and Dr. John S. Youtcheff, Jr., SaLUT, provided technical support during the course of the study. Dr. Williams is currently with Michigan Tech University, Houghton, MI. PURWheel tests were performed at Purdue University by Mr. Changlin Pan and Mr. James Stiady under the direction of Dr. Thomas D. White. Dr. White is currently with Mississippi State University, MS.

TABLE OF CONTENTS

Section	Page
CHAPTER 1: BACKGROUND	1
1. Introduction	1
2. Objectives	1
3. Structural Cross-Sections of the Pavements	2
4. Materials	2
a. Binders	5
b. Designations for the Binders and Mixtures Used in This Study	8
c. Aggregates	8
(1) Nominal Maximum Aggregate Size	8
(2) Aggregate Gradations and Types of Aggregates	9
(3) Flat, Elongated Particles	9
(4) Los Angeles Abrasion	14
(5) Fine Aggregate Angularity	14
5. Experimental Design for Testing the Pavements	14
a. Rutting Study	14
b. Fatigue-Cracking Study	16
6. Construction Report	17
7. Marshall Mixture Design Properties	17
a. Pre-Construction Marshall Mixture Designs	17
b. Marshall and Volumetric Properties Measured During and After Pavement Construction	19
8. Moisture Sensitivity	21
a. Pre-Construction Tests	21
b. Tests After Construction	21
9. Superpave Volumetric Properties	22
10. SGC Revolutions Needed to Obtain Air Voids That Matched the Final Air Voids of the Pavements	25
11. Confounding Factors in This Study	29
CHAPTER 2: VALIDATION OF THE SUPERPAVE BINDER PARAMETER FOR RUTTING BASED ON ALF PAVEMENT TESTS AT 58 °C	31
1. Superpave Binder Parameter for Rutting	31
a. Derivation of $G^*/\sin\delta$	31
b. $G^*/\sin\delta$'s of the Binders Corresponding to the ALF Pavement Tests	33
2. Background for the ALF Pavement Tests	34
3. ALF Pavement Tests Results at 58 °C	41
a. Temperature and Material Properties	41
b. Rut Depths	47
(1) Rut Depth vs. ALF Wheel Pass Relationships Using the Raw Data and a Rut Depth Model	47
(2) Comparison of the Rut Depth in the Asphalt Pavement Layer to the Total Rut Depth	47

(3) Statistical Rankings for the Pavements 48
(4) Comparisons of the Rut Depths at Various Wheel Passes ... 49
c. Pavement Cracks 50
4. Validation of G*/sinδ Based on the ALF Pavement Data From the Five Surface Mixtures 50
5. Validation of G*/Sinδ Based on the Data From the AC-5 and AC-20 (PG 59 and 70) Surface and Base Mixtures 50
a. Effect of Nominal Maximum Aggregate Size on Rutting Susceptibility 50
b. Interaction Between Nominal Maximum Aggregate Size and Grade of Binder 63
6. Evaluation of Other Binder Parameters 63
a. DSR Parameters From Sine Wave Tests 63
b. Zero Shear Viscosity 64
c. Cumulative Permanent Strain After Four Cycles of Repeated Loading 64
7. Properties of Binders Recovered From Pavement Cores 67
8. Conclusions 71
9. Comment on Binder Specifications 72

CHAPTER 3: VALIDATION OF THE SUPERPAVE BINDER PARAMETER FOR RUTTING BASED ON ALF PAVEMENT PERFORMANCE AT ALL TEST TEMPERATURES .. 73

1. Background 73
2. ALF Pavement Tests Results 73
a. Pavement Temperatures 73
b. Pavement Air Voids and Densification 73
c. Aggregate Gradation, Binder Contents, and Maximum Specific Gravity 74
d. Pavement Cracks 82
e. Pavement Rutting Data 82
3. Validation of G*/sinδ 83
4. Supplemental Analyses Performed on the ALF Pavement Data 93
a. Rut Depth in the Asphalt Pavement Layer vs. Total Rut Depth ... 93
b. Percentage of Rut Depth in Each Asphalt Pavement Lift 94
c. Evaluation of the Slopes and Intercepts From the Rut Depth vs. ALF Wheel Pass Relationships 94
(1) Introduction 94
(2) Slopes and Intercepts From the Gauss-Newton Model at a Test Temperatures of 58 °C 110
(3) Slopes and Intercepts From the Gauss-Newton Model at Test Temperatures of 58, 70, and 76 °C 111
(4) Slopes and Intercepts From the Gauss-Newton Model at Test Temperatures of 46, 52, and 58 °C 112
(5) Log-Log Rut Depth Model 112
(6) Interdependence of Slope and Intercept 112

5. Conclusions 115
a. Validation of $G^*/\sin\delta$ 115
b. Other Conclusions Provided by the ALF 115
c. Evaluation of the Slopes and Intercepts From the Rut Depth vs. ALF Wheel Pass Relationships 116
6. Final Discussion and Recommendations 117

CHAPTER 4: VALIDATION OF LABORATORY MIXTURE TESTS FOR RUTTING SUSCEPTIBILITY 118

1. Mixture Tests Evaluated 118
2. Short-term Oven Aging Study 119
3. Marshall Stability and Flow 120
4. GTM 120
5. French PRT 122
a. Description of the Equipment 122
b. Results From the French PRT 123
c. Comparison of the Rut Depths From the French PRT and ALF 130
d. Comparison of French PRT Data Using 50- and 100-mm-Thick Slabs 130
6. Georgia LWT 131
a. Description of the Equipment 131
b. Results From the Georgia LWT 132
7. Hamburg WTD 132
a. Description of the Equipment 132
b. Results From the Hamburg WTD 133
8. AAMAS 134
a. Description of the AAMAS Tests 134
b. AAMAS Analyses 135
c. Results From AAMAS 137
9. Repeated Load Compression Test 149
10. SST 150
a. Description of the SST 150
(1) Simple Shear 152
(2) Frequency Sweep 153
(3) Repeated Shear 153
b. Results From the SST for the Five Surface Mixtures at 40 °C 154
(1) Simple Shear 154
(2) Frequency Sweep 154
(3) Repeated Shear 154
c. Results From the SST for the Five Surface Mixtures at 58 °C 155
d. Results From the SST for the Surface vs. Base Mixture Study at 40 °C 155
e. Results From the SST for the Surface vs. Base Mixture Study at 58 °C 156
f. Results From the SST for the Surface vs. Base Mixture Study at 40 and 58 °C Using Specimens With a Diameter of 150 mm and a Height of 75 mm 156

g. Results From the SST for the Surface vs. Base Mixture Study at 40 and 58 °C Using Specimens With a Diameter of 203 mm and a Height of 75 mm 175
11. Tests Using the Purdue University Wheel Test Device (PURWheel) 175
a. Description of the Equipment 175
b. Results From the PURWheel 176
12. Comments on the Validation Effort 176
13. Supplementary Analysis: Shear Modulus vs. Compression Modulus 177
14. Conclusions 187
a. Surface Mixtures 187
b. Surface vs. Base Mixture Study (Four Mixtures Consisting of Two Gradations and Two Binders) 188
c. Conclusions Using All Mixtures 188
d. Miscellaneous Conclusions 189
15. Recommendations 190

CHAPTER 5: EFFECT OF COMPACTION METHOD ON RUTTING SUSCEPTIBILITY 191

1. Background and Objectives 191
2. French PRT 192
3. Georgia LWT 198
4. Hamburg WTD 198
5. SST Using Specimens With a Diameter of 150 mm 199
6. All Tests 204
7. SST Using Pavement Cores With a Diameter 203 mm 206
8. Conclusions 207

CHAPTER 6: G*/SINδ VERSUS LABORATORY MIXTURE TESTS FOR RUTTING 216

1. Background 216
2. French PRT, Georgia LWT, and Hamburg WTD 216
3. Repeated Load Compression Test 222
4. SST 222
5. Rankings Based on an Angular Frequency of 10.0 rad/s 223
6. Comment on Loading Time and Frequency 223
7. Conclusions 224
8. Recommendations 224

CHAPTER 7: EFFECT OF AGE HARDENING ON PAVEMENT RUTTING SUSCEPTIBILITY .. 229

1. Background and Objectives 229
2. Results and Conclusions for the Age-Hardening Study 229
3. Results and Conclusions for the Tire Pressure Study 230

CHAPTER 8: CONCLUSIONS AND RECOMMENDATIONS 237

1. Validation of G*/sinδ From the DSR Based on ALF Pavement Rutting Performance at 58 °C 237
2. Validation of G*/sinδ Based on ALF Pavement Rutting Performance at All Temperatures 238

3. Validation of Mixture Tests Based on the ALF Pavement Rutting Performances of the Five Surface Mixtures at 58 °C 239
4. Validation of Mixture Tests Based on the ALF Pavement Rutting Performances of the Surface and Base Mixtures With AC-5 and AC-20 (PG 59 and PG 70) at 58 °C 240
   a. Validation Using Laboratory-Prepared Specimens 240
   b. Validation Using Both Laboratory-Prepared and Pavement Specimens 241
5. Validation of Mixture Tests Based on the ALF Pavement Rutting Performances of All Seven Mixtures 241
6. Additional Conclusions Concerning the Laboratory Mixture Tests 242
7. Additional Conclusions Concerning the ALF Pavement Rutting Tests ... 243
8. Recommendations 243

REFERENCES 245

APPENDIX A: DESCRIPTIONS OF THE ACCELERATED LOADING FACILITY (ALF), SELECTED LABORATORY MIXTURE TESTS USED TO MEASURE RUTTING POTENTIAL, AND OF THE LINEAR KNEADING COMPACTOR 248

ALF Puts Superpave to the Test 249
U.S. Corps of Engineers Gyratory Testing Machine 254
French Pavement Rutting Tester 260
Georgia Loaded-Wheel Tester 264
Hamburg Wheel-Tracking Device 266
Superpave Shear Tester 272
Linear Kneading Compactor 276

APPENDIX B: AGGREGATE GRADATIONS, BINDER CONTENTS, AND MAXIMUM SPECIFIC GRAVITIES PROVIDED BY LOOSE MIXTURES ACQUIRED DURING CONSTRUCTION AND FROM PAVEMENT CORES TAKEN AFTER PAVEMENT FAILURE 279

APPENDIX C: ALF PAVEMENT RUT DEPTH DATA 291

1. Rut Depth Data 291
2. Downward Only Rut Depth vs. Peak-to-Valley Rut Depth 291

APPENDIX D: COMPARISON OF THE PERCENT PERMANENT STRAINS FROM VARIOUS TESTS 321

1. Test Data 321
2. Comment 323

APPENDIX E: MASTIC TESTS ON ALF MATERIALS 324

LIST OF FIGURES

Figure		Page
1.	Layout of the test lanes at the FHWA Pavement Testing Facility	3
2.	SM-3 aggregate gradation for the surface mixtures	12
3.	BM-3 aggregate gradation for the base mixtures	13
4.	G*/sinδ vs. temperature at a DSR frequency of 10.0 rad/s	36
5.	G*/sinδ vs. temperature at a DSR frequency of 2.25 rad/s	37
6.	The FHWA Accelerated Loading Facility and typical ruts in the pavements	38
7.	Close-up of the ALF super single tire and heat lamps on the right and left sides of the tire	39
8.	Thermocouple, core, and reference plate locations for each site	43
9.	Drawing of the reference rod used to measure the amount of rutting in the layers below the asphalt pavement layer	44
10.	Measured rut depth in the asphalt pavement layer vs. ALF wheel passes	51
11.	Rut depth in the asphalt pavement layer from the model vs. ALF wheel passes	52
12.	Measured total rut depth vs. ALF wheel passes	53
13.	Total rut depth from the model vs. ALF wheel passes	54
14.	Relationship between two times the standard deviation of the rut depth and the average rut depth	58
15.	ALF wheel passes at a 20-mm rut depth and 58 °C based on the rut depth model vs. G*/sinδ at 2.25 rad/s after RTFO	62
16.	Typical plot of applied DSR stress and resultant shear strain vs. time for the test consisting of a 1.0-s load duration followed by a 9.0-s rest period	68
17.	Example of pavement temperature vs. time (lane 7 site 2)	81
18.	Rut depths in asphalt pavement layer vs. ALF wheel passes using the Gauss-Newton model	85
19.	Rut depths in asphalt pavement layers with modified binders vs. ALF wheel passes using the Gauss-Newton model	86
20.	ALF wheel passes at a 20-mm rut depth based on the Gauss-Newton model for the five surface mixtures vs. G*/sinδ at 2.25 rad/s after RTFO	88
21.	ALF wheel passes at a 20-mm rut depth based on the measured data for the five surface mixtures vs. G*/sinδ at 2.25 rad/s after RTFO	89
22.	ALF wheel passes at a 10-mm rut depth due to viscous flow vs. G*/sinδ at 2.25 rad/s after RTFO	91
23.	Rut depth at 2,730 ALF wheel passes vs. G*/sinδ at 2.25 rad/s after RTFO	92
24.	ALF wheel passes at a 20-mm rut depth from the Gauss-Newton model vs. G*/sinδ at the pavement test temperature and 10 rad/s using binders recovered from wheelpath cores	98

25. ALF wheel passes at a 10-mm rut depth due to viscous flow vs. G*/sinδ at the pavement test temperature and 10 rad/s using binders recovered from wheelpath cores 99
26. ALF wheel passes at a 20-mm rut depth from the Gauss-Newton model vs. G*/sinδ at the pavement test temperature and 2.25 rad/s using binders recovered from wheelpath cores 101
27. ALF wheel passes at a 10-mm rut depth due to viscous flow vs. G*/sinδ at the pavement test temperature and 2.25 rad/s using binders recovered from wheelpath cores 102
28. Rut depth at 2,730 ALF wheel passes vs. G*/sinδ at the pavement test temperature and 2.25 rad/s using binders recovered from wheelpath cores 103
29. ALF wheel passes that provided a total rut depth of 20 mm vs. the ALF wheel passes that provided a rut depth of 20 mm in the asphalt pavement layer 104
30. ALF wheel passes that provided a total rut depth of 20 mm vs. ALF wheel passes that provided a rut depth of 20 mm in the asphalt pavement layer for the poorest performing mixtures 105
31. ALF wheel passes at a 20-mm rut depth vs. surface mixture 126
32. ALF wheel passes at a 20-mm rut depth vs. mixture type 126
33. Percent rut depth from the French PRT vs. surface mixture 126
34. Percent rut depth from the French PRT vs. mixture type 126
35. Rut depth from the Georgia LWT vs. surface mixture 127
36. Rut depth from the Georgia LWT vs. mixture type 127
37. Creep slope from the Hamburg WTD vs. surface mixture 127
38. Creep slope from the Hamburg WTD vs. mixture type 127
39. Instrumented specimen for the AAMAS repeated load and creep tests .. 138
40. Rutting potential chart for asphalt concrete surface layers 139
41. ALF wheel passes at a 20-mm rut depth vs. surface mixture 143
42. Stress at failure from the strength test vs. surface mixture 143
43. Strain at failure from the strength test vs. surface mixture 143
44. Creep modulus from the creep test vs. surface mixture 143
45. Total creep strain from the creep test vs. surface mixture 144
46. Permanent strain from the creep test vs. surface mixture 144
47. ALF wheel passes at a 20-mm rut depth vs. surface mixture 147
48. Cumulative permanent strain from the repeated load compression test vs. surface mixture 147
49. Dynamic modulus from the repeated load compression test vs. surface mixture 147
50. ALF wheel passes at a 20-mm rut depth vs. mixture type 148
51. Cumulative permanent strain from the repeated load compression test vs. mixture type 148
52. Dynamic modulus from the repeated load compression test vs. mixture type 148
53. Complex shear modulus, G*, at 40 °C 159
54. G*/sinδ at 40 °C 159
55. Complex shear modulus, G*, at 58 °C 161
56. G*/sinδ at 58 °C 161
57. ALF wheel passes at a 20-mm rut depth vs. mixture type 168
58. Cumulative permanent strain at 40 °C and 5,000 cycles 168

59. Maximum axial stress at 58 °C 168
60. Shear modulus vs. applied strain 183
61. Shear modulus vs. applied frequency 184
62. Coefficient of variation for the shear modulus vs. applied strain .. 185
63. Linear compression provided by the linear kneading compactor 195
64. Rut depths at 2,730 ALF wheel passes and from the wheel-tracking devices vs. $G^*/\sin\delta$ after RTFO 225
65. Rut depths at 10,000 ALF wheel passes and from the wheel-tracking devices vs. $G^*/\sin\delta$ after RTFO 226
66. Rut depth in the asphalt pavement layer from the model vs. ALF wheel passes for lane 9 233
67. Rut depth in the asphalt pavement layer from the model vs. ALF wheel passes for lane 10 234
68. Rut depth in the asphalt pavement layer from the model vs. ALF wheel passes for lane 11 235
69. Rut depth ±two standard deviation (±2STDV) at 58 °C 301
70. Measured rut depths in the asphalt pavement layer vs. ALF wheel passes 302
71. Measured rut depths in the asphalt pavement layer with modified binders vs. ALF wheel passes 303
72. Transverse profiles for lane 8, site 2, Novophalt (PG 77) surface mixture at 58 °C 304
73. Transverse profiles for lane 8, site 1, Novophalt (PG 77) surface mixture at 70 °C 305
74. Transverse profiles for lane 7, site 2, Styrelf (PG 88) surface mixture at 58 °C 306
75. Transverse profiles for lane 5, site 4, AC-10 (PG 65) surface mixture at 46 °C 307
76. Transverse profiles for lane 7, site 3, Styrelf (PG 88) surface mixture at 76 °C 308
77. Transverse profiles for lane 7, site 1, Styrelf (PG 88) surface mixture at 70 °C 309
78. Transverse profiles for lane 10, site 4, AC-20 (PG 70) surface mixture at 58 °C 310
79. Transverse profiles for lane 10, site 3, AC-20 (PG 70) surface mixture at 58 °C 311
80. Transverse profiles for lane 5, site 1, AC-10 (PG 65) surface mixture at 52 °C 312
81. Transverse profiles for lane 11, site 1, AC-5 (PG 59) base mixture at 58 °C 313
82. Transverse profiles for lane 6, site 2, AC-20 (PG 70) surface mixture at 64 °C 314
83. Transverse profiles for lane 10, site 1, AC-20 (PG 70) surface mixture at 58 °C 315
84. Transverse profiles for lane 10, site 2, AC-20 (PG 70) surface mixture at 58 °C 316
85. Transverse profiles for lane 5, site 2, AC-10 (PG 65) surface mixture at 58 °C 317
86. Gradations of the ALF aggregates and hydrated lime below 100 microns 328

LIST OF TABLES

Table Page

1. Pavement lanes for the Superpave validation study 4
2. Superpave PG's for the five binders 6
3. Pre-Superpave physical properties of the binders 7
4. Aggregate properties for the SM-3 surface mixtures 10
5. Aggregate properties for BM-3 base mixtures 11
6. Year when each pavement was tested for rutting susceptibility 15
7. Winter when each pavement was tested for fatigue-cracking susceptibility 15
8. Marshall mixture properties 20
9. Results from the ASTM D 4867 test method for moisture sensitivity performed on the five surface mixtures 23
10. Superpave Gyratory Compactor results 24
11. Number of Superpave gyratory revolutions needed to obtain the final pavement air-void levels 26
12. $G^*/\sin\delta$ after RTFO vs. temperature and angular frequency 35
13. High-temperature continuous PG at the standard DSR angular frequency of 10 rad/s and the ALF angular frequency of 2.25 rad/s 35
14. Pavement temperatures and air voids 45
15. $G^*/\sin\delta$ after RTFO corresponding to the ALF pavements tests 46
16. Pavement rankings based on the average ALF wheel passes needed to obtain rut depths of 15 and 20 mm using the raw data and the rut depth model 55
17. Average ALF pavement data 56
18. ALF replicate pavement data 57
19. Rankings for the pavements tested at 58 °C based on confidence bands for the rut depth vs. ALF wheel pass relationships 59
20. Rankings for the pavements tested at 58 °C based on the coefficient of variation (CV) 60
21. Rankings for the five surface mixtures at 58 °C based on $G^*/\sin\delta$ at 2.25 rad/s and ALF pavement performance 61
22. Binder parameters at 60 °C after RTFO 65
23. Additional tests on the five ALF binders at 60 °C 65
24. Cumulative permanent strain after four cycles of repeated loading using RTFO residues 69
25. Percent permanent strain for the 4th cycle of loading (Permanent Strain x 100 ÷ Total Strain) 69
26. Properties of binders recovered from cores taken from the wheelpath after performing the ALF pavement test for rutting 70
27. $G^*/\sin\delta$ after RTFO corresponding to the ALF pavements tests 75
28. Order in which the pavements were tested 76
29. ALF pavement data for the surface mixtures 77
30. Average pavement temperature (μ) and confidence limits ($\pm 2\sigma$) vs. pavement depth 80
31. Normalized percent pavement densification 80

32. ALF wheel passes based on the Gauss-Newton model that were needed to obtain rut depths of 10, 15, and 20 mm in the asphalt pavement layer 84
33. Final rut depths for the pavements tested for rutting 87
34. ALF wheel passes that provided a rut depth of 10 mm due to viscous flow, and rut depths in the asphalt pavement layer at 2,730 wheel passes 90
35. ALF wheel passes that were needed to obtain rut depths of 10, 15, and 20 mm in the asphalt pavement layer 95
36. High-temperature continuous PG based on a G*/sinδ of 2.20 kPa and an angular frequency of 10.0 rad/s 96
37. G*/sinδ of binders recovered from wheelpath cores at the pavement test temperature and an angular frequency of 10.0 rad/s 97
38. G*/sinδ of binders recovered from wheelpath cores at the pavement test temperature and an angular frequency of 2.25 rad/s 100
39. Percent rut depth in each lift with numerical and statistical ranking 106
40. Slopes and intercepts for rut depths in the asphalt pavement layer provided by the Gauss-Newton and log-log models 108
41. Slopes and intercepts for total rut depth provided by the Gauss-Newton and log-log models 109
42. Pavement rankings at 58 °C based on the average slope from the Gauss-Newton model and on $\pm 1\sigma_{(n-1)}$ and $\pm 2\sigma_{(n-1)}$ confidence bands for the slope 113
43. Pavement rankings at 58 °C based on the average slope from the log-log model and on $\pm 1\sigma_{(n-1)}$ and $\pm 2\sigma_{(n-1)}$ confidence bands for the slope 114
44. Short-term oven aging study 121
45. Rutting performance based on the Gyratory Testing Machine (GTM) at 60 °C 124
46. Rutting performance based on the French PRT, Georgia LWT, and Hamburg WTD 125
47. Statistical rankings for the five surface mixtures provided by the ALF and the three wheel-tracking devices 128
48. Statistical rankings for the surface and base mixtures provided by the ALF and the three wheel-tracking devices 128
49. Slopes and intercepts provided by the ALF and the French PRT 128
50 Rutting Susceptibility Based Upon the French PRT at 60 °C 129
51. Modified AAMAS traffic intensities 140
52. Rutting performance based on AAMAS, Modified AAMAS, and the repeated load compression test at 40 °C 141
53. Statistical rankings for selected AAMAS tests at 40 °C 145
54. Statistical rankings for the five surface mixtures provided by the ALF, the wheel-tracking devices, and repeated load compression test 145
55. Statistical rankings for the surface and base mixtures provided by the ALF, the wheel-tracking devices, and repeated load compression test 145
56. Rankings for the repeated load compression tests at 40 °C 146

57. ALF rutting performance vs. the repeated load compression test at 40 and 58 °C 151
58. SST results for the five surface mixtures at 40 °C 157
59. Statistical rankings for the five surface mixtures provided by the SST at 40 °C 158
60. SST results for the five surface mixtures at 58 °C 160
61. Statistical rankings for the five surface mixtures provided by the SST at 58 °C 162
62. Coefficients of variation in terms of percentages for the SST based on the data for the five surface mixtures 163
63. SST results for the surface and base mixtures at 40 °C 164
64. Statistical rankings for the surface and base mixtures provided by the SST at 40 °C 165
65. Non-statistical rankings for the surface and base mixtures provided by the SST at 40 °C 166
66. Results from *t*-tests showing the effect of nominal maximum aggregate size and the associated decrease on optimum binder content 169
67. SST results for surface and base mixtures at 58 °C 171
68. Statistical rankings for the surface and base mixtures provided by the SST at 58 °C 172
69. SST results at 40 °C for the surface and base mixtures using specimens prepared in the laboratory with a diameter of 150 mm and a height of 75 mm 173
70. SST results at 58 °C for the surface and base mixtures using specimens prepared in the laboratory with a diameter of 150 mm and a height of 75 mm 174
71. SST results at 40 °C for the surface and base mixtures using specimens prepared in the laboratory with a diameter of 203 mm and a height of 75 mm 179
72. SST results at 58 °C for the surface and base mixtures using specimens prepared in the laboratory with a diameter of 203 mm and a height of 75 mm 180
73. Rankings for the rut depths from the Purdue University Wheel Test Device (PURWheel) at 20,000 wheel passes and 58 °C 181
74. ALF rankings based on the number of wheel passes needed to obtain rut depths of 10, 15, and 20 mm in the asphalt pavement layer 181
75. Poisson's ratios at 40 °C for the seven mixtures calculated using the shear modulus from the SST and the resilient and dynamic moduli from the repeated load compression test 182
76. Poisson's ratios at 58 °C for the seven mixtures calculated using the shear modulus from the SST and the resilient and dynamic moduli from the repeated load compression test 186
77. Statistical rankings for the surface and base mixtures based on rutting susceptibility 193
78. Statistical rankings for the surface and base mixtures 194
79. Rut depths (mm) from the French PRT at 60 °C (data set #2) 194
80. Results from the French PRT at 60 °C and 30,000 cycles 196
81. Results from the French PRT at 60 °C and 10,000 cycles 196
82. Results from the Georgia LWT at 40 °C 200
83. Results from the Hamburg WTD at 50 °C 201

84. Average percent air voids of the specimens tested by the SST 201
85. SST data at 40 °C 202
86. Non-statistical rankings for the four mixtures based on the wheel-tracking devices 208
87. Statistical rankings for the four mixtures based on the wheel-tracking devices 209
88. Significant factors provided by three-way analyses of variance 210
89. Characteristics of the ALF and wheel-tracking tests 211
90. Non-statistical rankings for the four mixtures based on the SST at 40 °C 212
91. SST results using pavement cores with a diameter of 203 mm and a height of 50 mm for surface mixtures and 75 mm for base mixtures ... 213
92. Effect of specimen size and type on the SST results 214
93. High-temperature continuous PG's at 10 rad/s for the binders used in the surface vs. base mixture study 215
94. G*/sinδ and binder rankings at the angular frequencies and temperatures used in the ALF pavement and laboratory mixture tests . 217
95. Rut depths in the asphalt pavement layer at 2,370 and 10,000 ALF wheel passes 218
96. Rankings for the five surface mixtures vs. rankings based on the G*/sinδ's of the binders at the angular frequency and temperature corresponding to the ALF pavement and laboratory mixture tests 219
97. G*/sinδ and binder rankings at 10.0 rad/s and the temperatures used in the ALF pavement and laboratory wheel-tracking tests 227
98. Rankings for the five surface mixtures vs. rankings based on the G*/sinδ's of the binders at 10.0 rad/s and the temperature used in the ALF pavement and laboratory wheel-tracking tests 228
99. High-temperature continuous PG's at three different ages 231
100. G*/sinδ's at three different ages 231
101. ALF pavement data at 58 °C and three ages 232
102. Coefficient of determination, r^2, between the ALF wheel passes at rut depths of 10, 15, and 20 mm and the PG or G*/sinδ at 10 rad/s... 236
103. Aggregate gradations 280
104. Binder contents 289
105. Maximum specific gravities of the mixtures 290
106. Rut depth, Lane 5 Site 4 at 46 °C 293
107. Rut depth, Lane 3 Site 3 at 46 °C 293
108. Rut depth, Lane 5 Site 1 at 52 °C 294
109. Rut depth, Lane 6 Site 1 at 52 °C 294
110. Rut depth, Lane 9 Site 3 at 52 °C 294
111. Asphalt layer rut depth at 58 °C, mm, raw data 295
112. Asphalt layer rut depth at 58 °C, mm, model data 296
113. Total rut depth at 58 °C, mm, raw data 297
114. Total rut depth at 58 °C, mm, model data 298
115. Rut depth, Lane 6 Site 2 at 64 °C 299
116. Asphalt layer rut depth at 70 °C, mm 299
117. Total rut depth at 70 °C, mm 299
118. Asphalt layer rut depth at 76 °C, mm 300

119. Total rut depth at 76 °C, mm 300
120. ALF wheel passes at failure based on the downward only total rut depth and the peak-to-valley total rut depth 318
121. ALF wheel passes at failure based on the downward only rut depth and the peak-to-valley rut depth in the asphalt pavement layer alone ... 319
122. ALF wheel passes at failure for the Novophalt and Styrelf surface mixtures 320
123. Percent permanent strain per cycle of loading at 58 °C 321
124. Data from the ALF pavement tests at the 200th wheel pass 322
125. Data from the repeated load compression tests at the 200th cycle of loading 322
126. Comparison of the total strains in the tests (mm/mm) 323
127. Composition of the filler in the ALF pavements 327
128. G*/sinδ's of the unaged materials at 10.0 rad/s and 58 °C with 95-percent confidence limits ($\pm 2\sigma_{(n-1)}$) 329
129. Sine of the phase angle (sinδ) at 10.0 rad/s and 58 °C 330
130. G*/sinδ's of the unaged materials at 2.51 rad/s and 58 °C with 95-percent confidence limits ($\pm 2\sigma_{(n-1)}$) 331
131. Sine of the phase angle (sinδ) at 2.51 rad/s and 58 °C 332

CHAPTER 1: BACKGROUND

1. Introduction

This report documents a Federal Highway Administration (FHWA) study that was performed to assist the highway community in validating Superpave binder tests and specifications, Superpave mixture tests and performance models, and other laboratory tests that have been developed to predict the performances of asphalt mixtures. Twelve pavements were constructed in 1993 at the FHWA Pavement Testing Facility, located at the Turner-Fairbank Highway Research Center, McLean, VA, to assist in validating binder and mixture tests for rutting and fatigue cracking. Each pavement had a length of 44 m, a width of 4 m, and was divided into four test sites. Therefore, 48 sites were available for testing. The pavements were tested by the FHWA Accelerated Loading Facility (ALF), which is a full-scale, pavement testing machine that applies one-half of a single rear truck axle load. The pavements were tested under conditions that promoted either rutting or the formation of fatigue cracks. The variables used to control these conditions were pavement temperature, amount of lateral wheel wander, and load. At the time of this study, the FHWA owned two ALF's, which meant two sites could be tested at the same time. Figure 1 shows a layout of the pavements, designated as lanes 1 through 12.

2. Objectives

The objectives of the rutting study were to:

- Validate the Superpave binder parameter for rutting, $G^*/\sin\delta$, using ALF pavement performance.
- Validate laboratory mixture tests for rutting when operated according to standardized or customary procedures using ALF pavement performance.
- Compare rankings based on the Superpave binder parameter $G^*/\sin\delta$ to rankings provided by the laboratory mixture tests for rutting.
- Determine the effects of nominal maximum aggregate size on rutting susceptibility.
- Determine if the influence of binder high-temperature performance grade on rutting susceptibility decreases with an increase in nominal maximum aggregate size and the associated decrease in optimum binder content.

The objectives of the fatigue-cracking study were to:

- Validate the Superpave binder parameter for fatigue cracking, $G^*\sin\delta$, using ALF pavement performance.
- Validate the hypothesis stating that, when the tensile strain at the bottom of an asphalt pavement layer is high, a binder with a low stiffness will provide more resistance to fatigue cracking than a

binder with a high stiffness, and when the tensile strain is low, a binder with a high stiffness will provide more resistance to fatigue cracking than a binder with a low stiffness.

- Validate laboratory mixture tests for fatigue cracking using ALF pavement performance.

This chapter includes the experimental designs and background information for both the rutting and fatigue-cracking studies. The remaining chapters of this report detail the findings from the rutting studies. The findings from the fatigue-cracking studies will be presented in a separate report.

3. Structural Cross-Sections of the Pavements

The asphalt pavement layer in each of the 12 pavements consisted of a single asphalt mixture. It was placed on top of an unbound crushed aggregate base, so that rutting or fatigue-cracking performance would be a function of a single mixture. Table 1 shows that the asphalt pavement layer had a nominal thickness of 200 mm, except for lanes 1 and 2, which had a thickness of 100 mm. Lanes 1 and 2 were constructed for the fatigue-cracking studies; they were not used in the rutting studies. The thickness of the unbound crushed aggregate base layer was 460 mm, except for lanes 1 and 2 where the thickness was increased to 560 mm to account for the thinner asphalt pavement layer. The prepared subgrade had a thickness of 610 mm; its classification was A-4, based on American Association of State Highway Transportation Officials (AASHTO) Designation M 145-91.[1]

4. Materials

Table 1 shows that the asphalt mixtures consisted of five binders and two gradations. The two gradations consisted of a Virginia Department of Transportation (VDOT) surface mixture gradation designated SM-3 and a VDOT base mixture gradation designated BM-3.[2] The SM-3 and BM-3 gradations had nominal maximum aggregate sizes of 19.0 and 37.5 mm, respectively. The surface mixtures in lanes 1 and 2 were placed in two 50-mm lifts. The surface mixtures in lanes 3 through 10 were placed in four 50-mm lifts. The base mixtures in lanes 11 and 12 were placed in two 100-mm lifts.

For each gradation, the binder content was held constant so that the effects of binder properties on performance could be studied without the confounding effect of changes in binder content. No reclaimed asphalt pavement materials were included in the mixtures. Samples of the binders, aggregates, and hydrated lime were stockpiled at the Pavement Testing Facility during construction so that they could be used in laboratory experiments. Hydrated lime was used as an antistripping agent.

At the time when the materials for this project were chosen and the mixtures designed, the Superpave method of mixture design had not been finalized, nor had the operating specifications for the Superpave Gyratory Compactor (SGC). Therefore, the 75-blow Marshall method was used to design

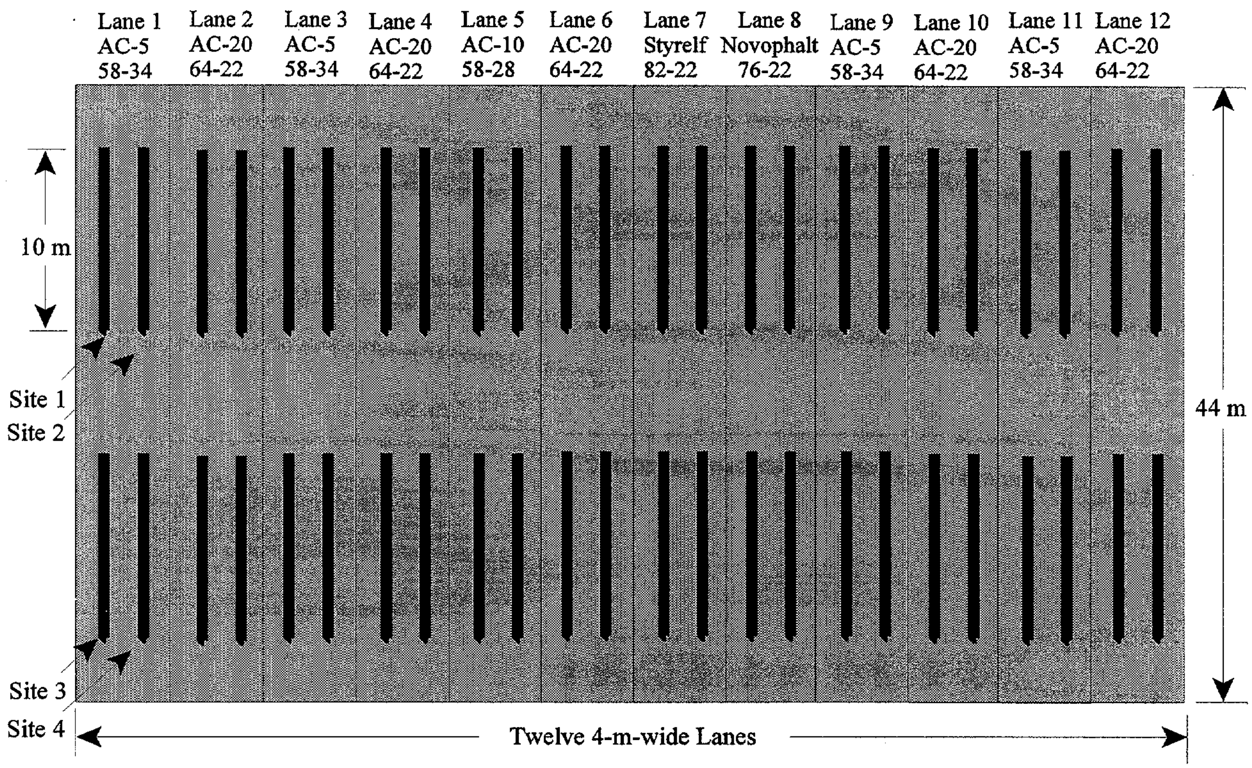

Figure 1. Layout of the test lanes at the FHWA Pavement Testing Facility.

Table 1. Pavement lanes for the Superpave validation study.

Lane Number	Characteristics of the Hot-Mix Asphalt Pavement Layer						Thickness of VDOT 21-A Unbound Crushed Aggregate Base Layer, mm	Thickness of AASHTO A-4 Uniform Subgrade, mm
	Layer Thickness, mm	VDOT Aggregate Gradation	Asphalt Binder Designation Prior to Superpave	Superpave Performance Grade (PG)	High-Temperature Continuous Grade After RTFO Aging	Intermediate Temperature Continuous Grade After RTFO & PAV		
1	100	SM-3	AC-5	58-34	59	9	560	610
2	100	SM-3	AC-20	64-22	70	17	560	610
3	200	SM-3	AC-5	58-34	59	9	460	610
4	200	SM-3	AC-20	64-22	70	17	460	610
5	200	SM-3	AC-10	58-28	65	15	460	610
6	200	SM-3	AC-20	64-22	70	17	460	610
7	200	SM-3	Styrelf™ I-D	82-22	88	18	460	610
8	200	SM-3	Novophalt™	76-22	77	20	460	610
9	200	SM-3	AC-5	58-34	59	9	460	610
10	200	SM-3	AC-20	64-22	70	17	460	610
11	200	BM-3	AC-5	58-34	59	9	460	610
12	200	BM-3	AC-20	64-22	70	17	460	610

the mixtures. However, the asphalt binders and aggregates were chosen based on the Superpave specifications at the time of construction.

a. Binders

The designations of the five binders prior to the Superpave Performance Grade system were AC-5, AC-10, AC-20, Novophalt™, and Styrelf™I-D. The AC-5, AC-10, and AC-20 were from Venezuela's Lagoven base stock. The Novophalt binder was formulated by blending the Lagoven AC-10 asphalt with 6.5-percent low-density polyethylene by mass. A high shear mill was used for blending. Blending was performed by Advanced Asphalt Technologies, Sterling, Virginia, at the paving contractor's hot-mix plant in Leesburg, Virginia. The Styrelf I-D binder was formulated by reacting the Lagoven AC-20 asphalt with 4-percent styrene-butadiene by volume. Styrelf is a product of the Koch Materials Company and is shipped in bulk form. Styrelf binders are currently called Styflex™ in the United States.

Table 2 shows that the Superpave Performance Grades (PG's) of the binders were 58-34, 58-28, 64-22, 76-22, and 82-22. These PG's were determined in accordance with 1993 and 1994 AASHTO provisional standards that were assembled and published in 1995.(3) The two modified binders were chosen to provide different high-temperature PG's, not to directly compete against each other.

The continuous PG is defined as the temperature at the specified test criterion, for example, the temperature at a $G^*/\sin\delta$ of 2.20 kPa after aging in a rolling thin-film oven (RTFO). Table 2 shows that the high-temperature continuous PG's for rutting performance, based on testing RTFO residues, were 59, 65, 70, 77, and 88. The intermediate-temperature continuous PG's for fatigue-cracking performance, based on testing rolling thin-film oven/pressure aging vessel (RFTO/PAV) residues, were 9, 15, 17, 20, and 18. The interval between PG's is 6 °C for high-temperature performance and 3 °C for intermediate-temperature performance.

The physical binder properties based on the viscosity grading system are shown in table 3. These properties were determined using AASHTO test methods.(4) The penetration and viscosity tests ranked the binders the same as the high-temperature PG's in table 2. The absolute viscosities of the Styrelf binder at 60 °C could be in error. These viscosities were difficult to obtain because they were very high. The PG system circumvents testing problems associated with using a constant temperature by specifying a required physical property that is related to performance. The temperature needed to obtain this property is then determined. Thus, binders are not tested at widely different rheological states as in the viscosity test.

Although viscosity is a fundamental measurement, it does not describe both elastic (recoverable) and viscous (permanent) deformations, whereas both deformations occur in pavements. The Dynamic Shear Rheometer (DSR) does provide a measure of both deformations. The viscosity test at 60 °C also does not provide intermediate- and low-temperature properties that are needed to rate or rank binders in terms of fatigue and thermal cracking. The

Table 2. Superpave PG's for the five binders.

Pre-Superpave Designation:	AC-5	AC-10	AC-20	Novo-phalt	Styrelf
Superpave PG:	58-34	58-28	64-22	76-22	82-22
Original Binder					
Temperature at G*/sinδ of 1.00 kPa and 10 rad/s, °C	59.4	61.9	67.9	77.3	87.2
RTFO Residue					
Temperature at G*/sinδ of 2.20 kPa and 10 rad/s, °C	59.3	65.0	70.2	76.6	88.0
RTFO/PAV Residue					
Temperature at G*sinδ of 5000 kPa and 10 rad/s, °C	9.1	14.7	16.7	20.0	17.7
Temperature at Creep Stiffness (S) of 300 MPa and 60 s, °C	-26.9	-22.1	-19.8	-19.7	-20.9
Temperature at an m-value of 0.30 and 60 s, °C	-25.3	-20.3	-17.1	-13.6	-17.4
Continuous PG's Using Samples Taken During Construction[1]					
PG at Start of Construction, Lab A	58-36	61-31	68-34	76-25	89-30
PG at Middle of Construction, Lab A	58-36	62-33	68-28	83-22	87-29
PG at End of Construction, Lab A	63-34	62-31	67-33	77-24	87-28
PG at End of Construction, Lab B	59-35	62-30	68-27	76-23	87-27

[1]The low-temperature PG is the temperature provided by the Superpave bending beam test plus 10 °C.

Table 3. Pre-Superpave physical properties of the binders.

Virgin Binder	AC-5	AC-10	AC-20	Novo-phalt	Styrelf
Penetration, 25 °C, 0.1 mm	172	113	73	54	47
Absolute Viscosity, 60 °C, dPa·s	665	1 195	2 644	13 814	60 308
Kinematic Viscosity, 135 °C, mm^2/s	256	322	476	2 184	2 484
Specific Gravity, 25/25 °C	1.007	1.024	1.022	1.022	1.020
Solubility in Trichloroethylene, %	100.00	100.00	100.00	95.92	100.00
Flash Point, COC, °C	304	304	304	326	312
Thin-Film Oven Residue					
Mass Loss, %	0.01	0.33	0.13	0.34	0.12
Penetration, 25 °C, 0.1 mm	102	66	47	40	35
Absolute Viscosity, 60 °C, dPa·s	1 758	3 223	7 183	29 844	208 185
Kinematic Viscosity, 135 °C, mm^2/s	372	509	684	3 686	4 197

susceptibility to cracking is assumed to increase as the viscosity at 60 °C increases, or the viscosity and penetration of a binder are used together to try to control cracking. The penetration test is performed at intermediate temperatures, generally 25 °C, but, like the viscosity test, it does not describe both elastic and viscous deformations. It is an empirical test that often cannot be related to the various pavement distress modes.

b. Designations for the Binders and Mixtures Used in This Study

During the course of this study, it was decided to describe the five binders using the viscosity grading system and the modifier trade names because of discrepancies that arose between the PG's and the pavement performances of the two mixtures with the modified binders. These descriptions are termed "Pre-Superpave." Discrepancies provided by modified binders are unique to the particular type of modification that is used, and the inability of the binder tests to properly characterize them. A discrepancy does not mean that the PG system is in error for most binders, or that the temperature increment between the PG's is incorrect. Therefore, trade names should be used to describe modified binders that do not fit the current PG system.

In the text of this report, the pre-Superpave designations for the five binders are given for each unmodified binder followed by the PG when general information about the binder is given. The high-temperature continuous PG at 10 rad/s and 2.20 kPa after RTFO aging is used in discussions specific to the rutting study. Only the trade names are given for the two modified binders. The pre-Superpave designation is always used in tables; in some cases, the PG is also included.

c. Aggregates

(1) Nominal Maximum Aggregate Size

All five binders were used with a VDOT SM-3 surface mixture gradation that had a nominal maximum aggregate size of 19.0 mm.[2] Nominal maximum aggregate size was based on the Superpave definition, which states that the nominal maximum aggregate size is one sieve size larger than the first sieve to retain more than 10 percent aggregate by mass.[5] A nominal maximum aggregate size of 12.5 mm is more commonly used in surface mixtures, but the larger size was chosen based on the assumption that the high temperatures and loads to be used in the pavement rutting tests would be too severe for typical VDOT surface mixtures having a nominal maximum aggregate size of 12.5 mm.

The AC-5 and AC-20 (PG 58-34 and 64-22) binders were also used with a VDOT BM-3 base mixture gradation that had a nominal maximum aggregate size of 37.5 mm. Table 1 shows that these two mixtures were placed in lanes 11 and 12. The surface and base mixtures with AC-20 (PG 64-22) are used in Northern Virginia highways subjected to heavy traffic levels, and they are highly resistant to rutting when properly designed and constructed. The aggregates were also used in pavements tested by the FHWA ALF in previous FHWA studies, but the gradations were different.

(2) Aggregate Gradations and Types of Aggregates

The aggregate gradations met 1991 VDOT specifications.[2] The gradation for the surface mixture also met VDOT specifications for an intermediate mixture, designated as IM. Tables 4 and 5 show the "target" gradations for mixtures prepared in the laboratory. These were based on the average gradations of the mixtures in the pavements. The "lab blend" gradations were the actual gradations used in laboratory mixtures. Aggregates in the laboratory were sieved down to the 1.18-mm sieve size. The aggregates were then blended to meet the target gradations as closely as possible. The target gradations are also shown in figures 2 and 3 along with the Superpave control limits.

Different sources of diabase were used in the two gradations, a fact that was not known until the time of construction. The diabase used in the surface mixtures was from Virginia Trap Rock, Leesburg, Virginia, while the diabase used in the base mixtures was from Luck Stone, Leesburg, Virginia. Both were 100-crushed, quarried aggregates from the same geologic vein. Neither aggregate source contained particles with rounded surfaces or clays. Prior to this study, the paving contractor used diabase from the Virginia Trap Rock quarry because this quarry was located next to the hot-mix plant. The paving contractor had stockpiles of this aggregate at the plant at the time of construction. However, neither the paving contractor nor Virginia Trap Rock had the No. 357 stone needed for the base mixture. Therefore, the paving contractor obtained the diabase aggregates for the base mixtures from Luck Stone.

A natural sand from the Solite Corporation, Fredericksburg, Virginia, was used in both mixtures. This sand is predominantly quartz and quartzite. One-percent hydrated lime, purchased from Chemston, Strasburg, Virginia, was used in all mixtures to prevent the occurrence of moisture damage during the duration of this study.

(3) Flat, Elongated Particles

The aggregates were tested for flat and elongated particles using ASTM D 4791.[6] At the time of construction, Superpave specified that a maximum of 10 percent particles by mass could pass a 5 to 1, length-to-thickness, ratio.[5] It was found that less than 1 percent of the diabase aggregates had a length to thickness greater than this ratio. The aggregates easily passed the Superpave specification.

A length-to-thickness ratio of 3 to 1 was also used to evaluate the aggregates. A maximum value of 20 percent using a 3-to-1 ratio has been used by some highway agencies in the past, although a firm criterion does not exist. The No. 68 diabase aggregate in the surface mixtures had an average percent passing of 21. The No. 357 and No. 8 diabase aggregates in the base mixtures had average percent passing of 19 and 12, respectively. The No. 68 and No. 357 diabase aggregates had a moderate number of flat and elongated particles based on a 3-to-1 ratio.

Table 4. Aggregate properties for the SM-3 surface mixtures.

Aggregate Gradations, Percent Passing:

Sieve Size (mm)	61% No. 68 Diabase	30% No. 10 Diabase	8% Natural Sand	1% Hydrated Lime	Target	Lab Blend
25.0	100.0				100.0	100.0
19.0	97.9				98.7	98.7
12.5	60.7				76.0	76.0
9.5	37.7	100.0	100.0		62.0	62.0
4.75	9.2	99.2	95.8		44.0	44.0
2.36	2.2	75.6	88.2		32.5	32.1
1.18	1.7	52.5	74.8		23.5	23.8
0.600	1.4	37.8	46.0		17.5	16.9
0.300	1.3	27.9	14.1		11.5	11.3
0.150	1.1	19.6	4.8		8.0	7.9
0.075	0.9	12.5	2.9	100.0	5.1	5.5

The diabase aggregates were from Virginia Trap Rock.

Specific Gravities and Percent Absorption:

	61% No. 68 Diabase	30% No. 10 Diabase	8% Natural Sand	1% Hydrated Lime	Target	Lab Blend
Bulk Dry	2.943	2.914	2.565			2.892
Bulk SSD	2.962	2.945	2.601			2.916
Apparent	2.999	3.007	2.659	2.262		2.961
% Abs	0.6	1.1	1.4			0.8

Flat and Elongated Particles at a 3-to-1 Length-to-Thickness Ratio, Percent by Mass:

61% No. 68 Diabase	30% No. 10 Diabase	8% Natural Sand
21	NT	NT

Los Angeles Abrasion, Percent Loss by Mass:

61% No. 68 Diabase	30% No. 10 Diabase	8% Natural Sand
14	NT	NT

Bulk Dry = Bulk-Dry Specific Gravity
Bulk SSD = Bulk-Saturated-Surface-Dry Specific Gravity
Apparent = Apparent Specific Gravity
% Abs = Percent Water Absorption
NT = Not Tested

Table 5. Aggregate properties for BM-3 base mixtures.

Aggregate Gradations, Percent Passing:

Sieve Size (mm)	41% No. 357 Diabase	15% No. 8 Diabase	38% No. 10 Diabase	5% Natural Sand	1% Hydrated Lime	Target	Lab Blend
37.5	100.0					100.0	100.0
25.0	64.9					85.6	85.6
19.0	36.3					73.9	73.9
12.5	14.9	100.0				65.1	65.1
9.5	5.5	85.0	100.0	100.0		59.0	59.0
4.75	3.0	25.3	96.8	95.8		47.6	47.6
2.36	1.8	2.7	68.0	88.2		32.5	32.4
1.18	1.6	2.0	47.5	74.8		24.0	23.7
0.600	1.4	1.5	34.3	46.0		17.4	17.1
0.300	1.2	1.2	24.9	14.1		12.3	11.8
0.150	1.1	0.9	17.3	4.8		8.0	8.4
0.075	0.8	0.8	11.5	2.9	100.0	5.7	6.0

The diabase aggregates were from Luck Stone Corporation.

Specific Gravities and Percent Absorption:

	41% No. 357 Diabase	15% No. 8 Diabase	38% No. 10 Diabase	5% Natural Sand	1% Hydrated Lime	Target	Lab Blend
Bulk Dry	2.971	2.956	2.894	2.565			2.907
Bulk SSD	2.984	2.981	2.935	2.601			2.934
Apparent	3.013	3.030	3.017	2.659	2.262		2.987
% Abs	0.5	0.8	1.4	1.4			0.9

Flat and Elongated Particles at a 3-to-1 Length-to-Thickness Ratio, Percent by Mass:

	41% No. 357 Diabase	15% No. 8 Diabase	38% No. 10 Diabase	5% Natural Sand
	19	12	NT	NT

Los Angeles Abrasion, Percent Loss by Mass:

	41% No. 357 Diabase	15% No. 8 Diabase	38% No. 10 Diabase	5% Natural Sand
	20	21	NT	NT

Bulk Dry = Bulk-Dry Specific Gravity.
Bulk SSD = Bulk-Saturated-Surface-Dry Specific Gravity.
Apparent = Apparent Specific Gravity.
% Abs = Percent Water Absorption.

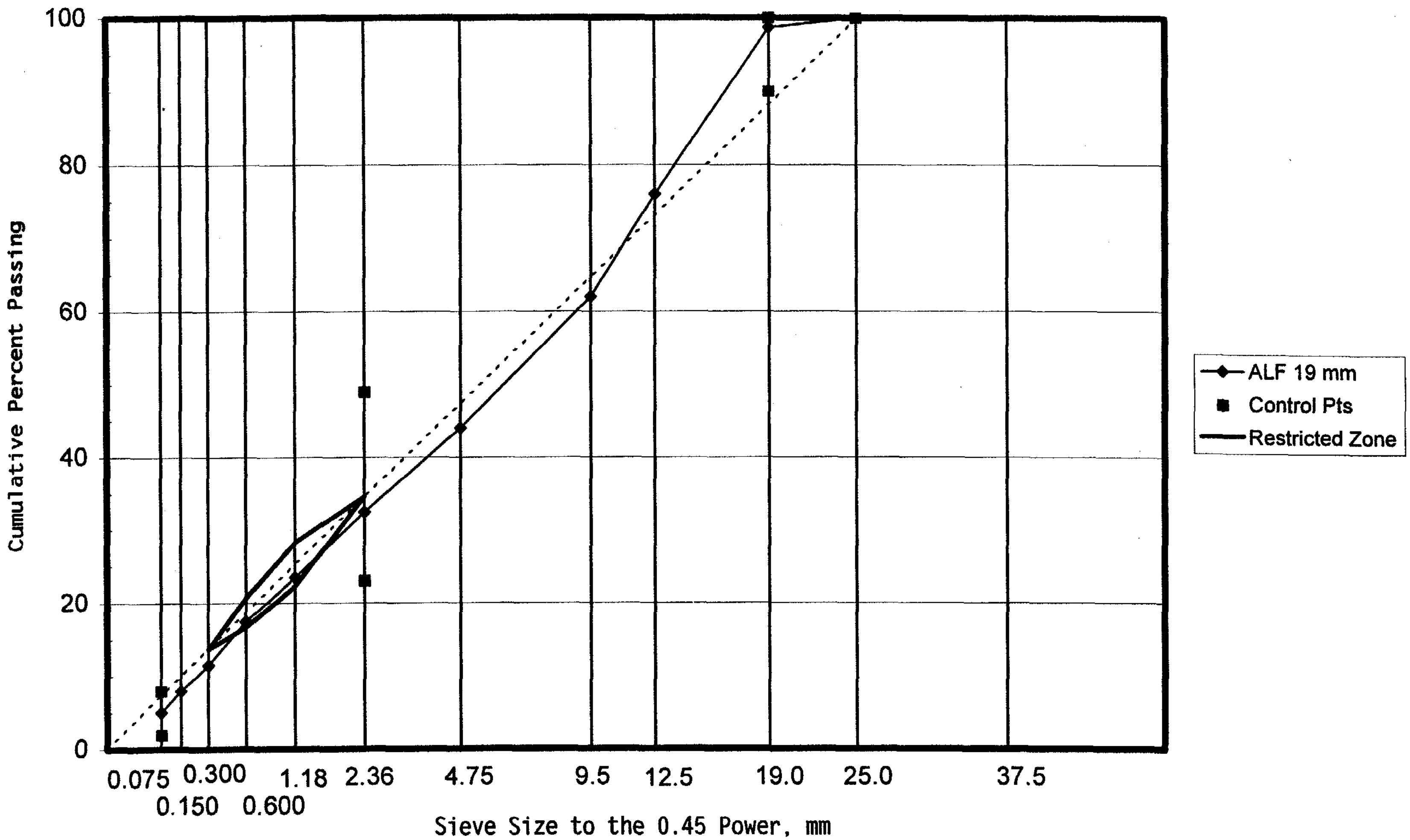

Figure 2. SM-3 aggregate gradation for the surface mixtures.

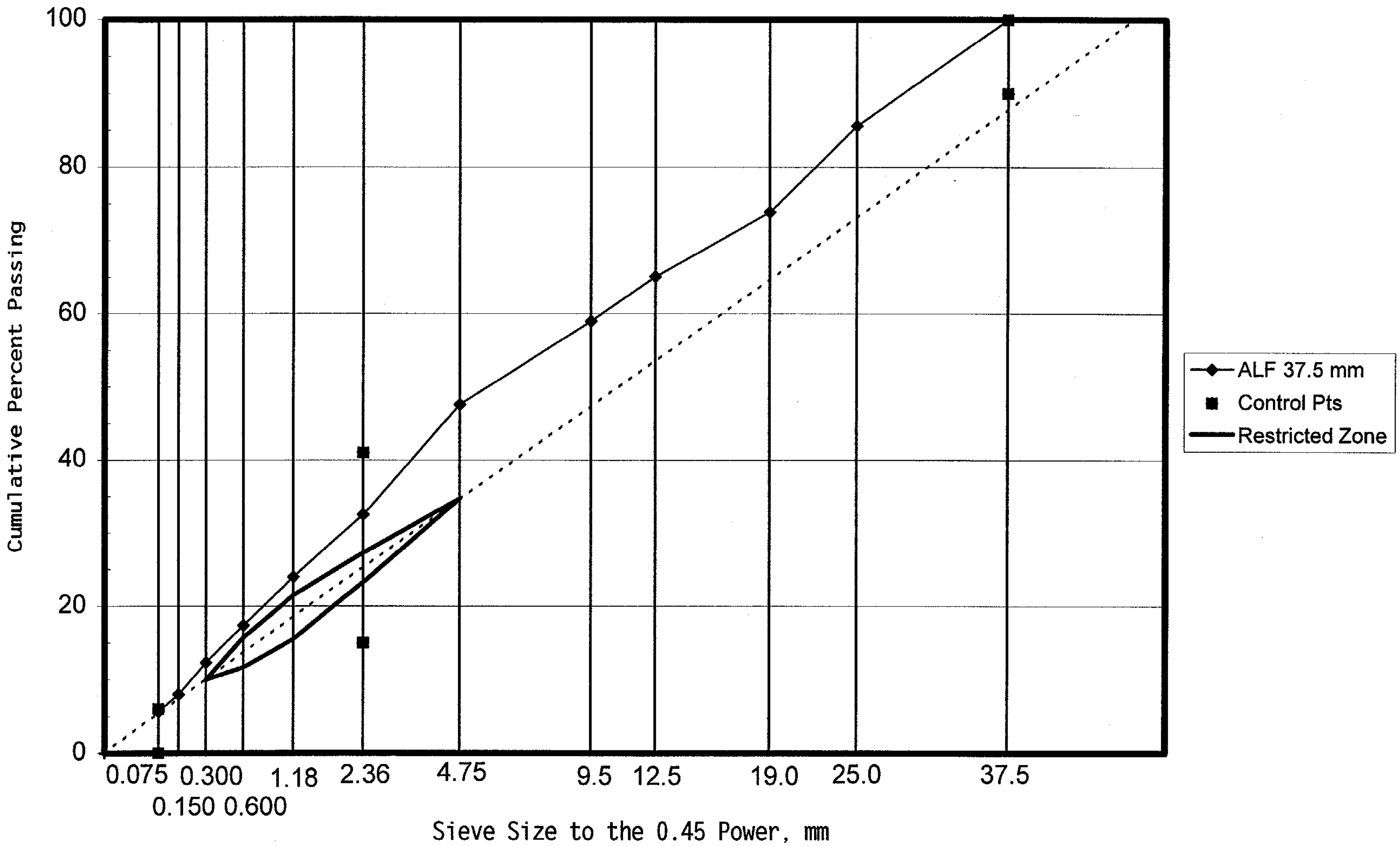

Figure 3. BM-3 aggregate gradation for the base mixtures.

(4) Los Angeles Abrasion

The No. 68 diabase aggregate in the surface mixtures had an average Los Angeles abrasion of 14 when tested in accordance with AASHTO T 96.[4] The No. 357 and No. 8 diabase aggregates in the base mixtures had average Los Angeles abrasions of 20 and 21, respectively. These values indicated that the diabase aggregates were highly resistant to abrasion. Maximum allowable losses are typically in the range of 35 to 40.[5]

(5) Fine Aggregate Angularity

Fine aggregate angularities were measured using the National Aggregate Association's Method A, which was the predecessor of AASHTO TP33-93.[3,7] This method evaluates shape and texture in terms of the percentage of voids in a dry, uncompacted sample. A high void level usually indicates high angularity and a rough texture. A low void level usually indicates the material is rounded and smooth. The 2.36- to 0.150-mm fraction of each fine aggregate was tested.

The No. 10 diabase from Virginia Trap Rock, No. 10 diabase from Luck Stone, and the natural sand from Solite had fine aggregate angularities of 49, 48, and 45 percent, respectively. Superpave required a minimum value of 45 percent for the combined fine aggregate used in surface mixtures that will have traffic levels equal to and greater than 3 million equivalent single axle loads (ESAL's).[5] All three materials individually passed this specification, indicating they had moderate to high angularities and roughnesses. The two diabase aggregates had statistically higher fine aggregate angularities than the natural sand, indicating some slight difference in the materials. Microscopic analyses indicated that particles in the larger size fractions of the natural sand were slightly more cubic in shape than the particles in the diabase aggregates. The diabase aggregates had more elongated particles.

5. Experimental Design for Testing the Pavements

a. Rutting Study

The ALF pavement tests for rutting, including the year that each test was performed, are shown in table 6. Each surface mixture was tested for rutting susceptibility at three pavement temperatures to determine the relationship between rut depth and temperature. The overall temperature range was 46 to 76 °C. The only pavement temperature that could be used for all seven mixtures was 58 °C. The large differences in rutting performance from mixture to mixture, coupled with large changes in rutting performance with a change in temperature, prohibited testing all seven mixtures at another single temperature. The pavements would either rut too quickly or not rut at all, using another single temperature. All seven mixtures were tested at 58 °C in 1994. Tests at 58 °C were repeated in 1995 on the pavements with the

Table 6. Year when each pavement was tested for rutting susceptibility.

Mixture	Pavement Test Temperature and Year of Test							
	46 °C	52 °C	58 °C	58 °C	58 °C	64 °C	70 °C	76 °C
AC-5	1997	1997	1994	1995	1998			
AC-10	1997	1996	1994					
AC-20		1996	1994	1995	1998	1997		
Styrelf			1994				1995	1997
Novophalt			1994				1995	1997
AC-5 Base			1994	1995	1998			
AC-20 Base			1994					

Table 7. Winter when each pavement was tested for fatigue-cracking susceptibility.

Lane	Mixture	Layer Thickness	Pavement Test Temperature and Year of Test		
			28 °C	19 °C	10 °C
1	AC-5	100 mm	1994 to 1995	1997 to 1998	1997 to 1998
2	AC-20	100 mm	1994 to 1995	1997 to 1998	1997 to 1998
3	AC-5	200 mm	1995 to 1996	1996 to 1997	1999 to 2000
4	AC-20	200 mm	1995 to 1996	1996 to 1997	2000 to 2001
5	AC-10	200 mm			1999 to 2000
6	AC-20	200 mm			2000 to 2001
7	Styrelf	200 mm			2000 to 2001
8	Novophalt	200 mm			2000 to 2001

AC-5 and AC-20 (PG 59 and 70) surface mixtures and the AC-5 (PG 59) base mixture to determine the repeatability of the ALF data. These pavements were tested again in 1998 to evaluate age hardening.

Lanes 9, 10, 11, and 12 were dedicated to the rutting study with the objective of determining the effect of nominal maximum aggregate size on rutting susceptibility. Table 1 shows that lanes 9 and 11 contained the AC-5 (PG 59) binder, while lanes 10 and 12 contained the AC-20 (PG 70) binder. The hypothesis to be evaluated was that an increase in nominal maximum aggregate size would decrease the optimum binder content and increase the resistance to rutting.

Another objective was to determine whether the influence of binder grade on rutting susceptibility decreases with an increase in nominal maximum aggregate size. This was to be accomplished by determining the difference in rutting susceptibility provided by the two binders at each nominal maximum aggregate size. The effects for each nominal maximum aggregate size could then be compared with each other. It was hypothesized that binder grade would have less effect on rutting susceptibility when using the larger nominal maximum aggregate size and lower binder content.

Lane 6 with the AC-20 (PG 70) surface mixture was an extra lane. It was constructed in case it was perceived that a pavement should be tested at the same time as a control pavement. The AC-20 (PG 70) surface mixture was considered the control mixture. Fluctuating pavement temperatures or changes in the properties of the underlying materials might lead to a decision that a pavement and a control pavement needed to be tested at the same time using both ALF's. The additional lane provided four additional test sites.

b. Fatigue-cracking Study

The ALF pavement tests for fatigue cracking, including the year that each test was performed, are shown in table 7. Lanes 1, 2, 3, and 4 were dedicated to the fatigue-cracking study with the objective of evaluating possible interactions between asphalt pavement layer thickness, binder grade, and temperature. The primary hypothesis to be evaluated was that softer binders perform better when the asphalt pavement layer is subjected to relatively high tensile strains, while stiffer binders perform better when the asphalt pavement layer is subjected to relatively low tensile strains.

Table 7 shows that temperatures of 28, 19, and 10 °C were used to determine the relationship between fatigue cracking and temperature for the study involving asphalt pavement layer thickness. For these experiments, the pavements were tested in pairs using both ALF's to minimize the effect that changes in the properties of the underlying materials with time might provide. Lane 1 was tested at the same time as lane 2, and lane 3 was tested at the same time as lane 4.

6. Construction Report

Details on the construction of the asphalt pavement layers are documented in a separate report.[8] All binder, aggregate, and mixture tests were performed according to AASHTO test methods.[4] The construction report includes the following:

- Binder test data collected to ensure that the properties of the binders did not change while they were being used. Binder samples were obtained during the mixture designs, from the terminal immediately before shipping, from the hot-mix plant after they arrived from the terminal, and daily during construction. The properties measured were viscosity at 135 °C using a Brookfield viscometer, $G^*/\sin\delta$ at 20 °C and 10 rad/s using the DSR, and infrared analysis, which was used to monitor the functional groups (chemistry) of the binders.

- Marshall mixture design data.

- Comparisons between design and as-constructed properties of the mixes, including aggregate gradations, natural sand contents, binder contents, air voids, and the maximum specific gravities of the mixtures.

- Quality control testing conducted by the paving contractor (binder content, aggregate gradation, nuclear density, maximum specific gravity, and pavement thickness), and quality assurance testing by the FHWA to make sure the specifications of the project were met.

As an example of the data collected during construction, and because of the importance of binder properties to this study, Superpave continuous PG's for samples taken at the start, middle, and end of construction are included in table 2. The high-temperature continuous PG's in table 2 are the temperatures at a $G^*/\sin\delta$ of 1.00 kPa using original, unaged binders. The low-temperature continuous PG's are the temperatures at an m-value of 0.300 plus 10 °C using RTFO/PAV residues. The full suite of Superpave binder tests was not performed on these samples.

The properties of the binders were generally consistent. The low-temperature continuous PG for the AC-20 (PG 64-22) binder provided the greatest amount of variability, ranging from -27 to -34 °C. This spans more than one PG. For low-temperature performance, the interval between PG's is 6 °C. Additional tests on this binder showed the low-temperature continuous PG to be approximately -28 °C.

7. Marshall Mixture Design Properties

a. Pre-Construction Marshall Mixture Designs

The 75-blow Marshall method was used to design the five SM-3 surface mixtures prior to construction.[2,4,9] The following VDOT mixture design criteria were used:

- 75 blows per side using a 4.536-kg hammer.
- Specimen diameter of 101.6 mm and thickness of 63.5 mm.
- Optimum binder content at 4-percent total air voids.
- Minimum stability of 8006 N.
- Flow between 8 and 14, except for the Novophalt and Styrelf mixtures. where only a minimum flow of 8 was required.
- Minimum Voids in the Mineral Aggregate (VMA) of 14.0.
- Voids Filled With Asphalt (VFA) between 65 and 80 percent.

A 112-blow Marshall method was used to design the two BM-3 base mixtures.[10] The stabilities in this method were divided by 2.25, while the flows were divided by 1.5. Theoretically, this conversion accounts for the larger sized specimen used in the 112-blow method compared with the 75-blow method. After converting the data, the data from the two procedures can be compared against each other, and the pass-fail criteria for the 75-blow method can be applied to data from the 112-blow method. Mixture design criteria were as follows:

- 112 blows per side using a 10.21-kg hammer.
- Specimen diameter of 152.4 mm and thickness of 95.3 mm.
- Optimum binder content at 4-percent air voids.
- Minimum stability of 8006 N based on a specimen diameter of 101.6 mm and thickness of 63.5 mm.
- Flow between 8 and 14 based on a specimen diameter of 101.6 mm and thickness of 63.5 mm.
- Minimum VMA of 12.0.
- VFA between 65 and 80 percent.

The average optimum binder contents for the surface and base mixtures were 4.9 and 4.0 percent by mass, respectively. These binder contents provided air-void levels in the range of 4 ±1 percent. All mixtures had Marshall stabilities above 11 000 N. A minimum level of 8006 N is required for pavement mixtures that will have heavy traffic levels. All mixture design criteria were met.

The dust-to-binder ratio by mass was specified by Superpave to be in the range of 0.6 to 1.2[5], although at the time of this report, AASHTO was to vote on raising the upper limit to 1.5 or 1.6. Dust is defined as the percent aggregate by mass passing the 0.075-mm sieve. Binder is defined as the effective binder content by mass (non-absorbed binder). The total binder content by mass was used prior to Superpave when calculating the ratio. Superpave changed the definition for binder, but did not change the definition for dust or the criteria. The total binder content was used when designing the mixtures for this study, although no data existed showing the applicability of the criteria to the mixtures being evaluated. The surface and base mixtures had average ratios of 1.0 and 1.2, respectively, using total binder content, and average ratios of 1.2 and 1.3 using the effective binder content. Additional details for the designs are documented in the construction report.[8]

b. Marshall and Volumetric Properties Measured During and After Pavement Construction

Marshall and volumetric properties for loose mixtures sampled and compacted during construction are given in table 8. Included in table 8 are the properties for mixtures prepared using the stockpiled materials. Binder contents of 4.85 and 4.00 were used in the latter mixtures. These were the overall average binder contents for the two types of mixtures. They were based on the results of extractions performed on samples of loose mixtures taken from the trucks during construction and on pavement cores.[8] Average gradations, shown in tables 4 and 5, were used in these mixtures.

The data in table 8, along with the gradations collected during construction, indicated that the plant-produced mixtures and laboratory-produced mixtures were essentially the same. For example, the air voids ranged from 2.5 to 4.1 percent for the plant-produced mixtures and from 2.9 to 4.3 percent for the laboratory-produced mixtures. The differences between the sets of data are most likely related to small differences in the compositions of the mixtures and to differences in short-term aging. The plant-produced loose mixtures were not oven-aged in the laboratory, while the laboratory-produced loose mixtures were oven-aged at 135 °C for 2 h before compaction. The development of the 2-h oven-aging period is discussed in chapter 2.

The data in table 8 show that the air voids for the AC-5, AC-10, and AC-20 (PG 58-34, 58-22, and 64-22) surface mixtures tended to be low, while their Marshall flows tended to be high. The air voids should be close to 4.0 percent. The maximum Marshall flow was specified to be 14 for these three mixtures. However, the paving contractor was not required to use Marshall or volumetric properties for process control in this project, and at the time of construction, this type of process control was not required by VDOT.

The Marshall stabilities and flows were examined statistically.[11] There were no statistically significant differences between most of the stabilities. The differences among the average stabilities were relatively small compared with the variability of the replicate measurements. Only the mixtures with the highest and lowest stabilities had significantly different stabilities.

In summary, all mixtures had stabilities significantly above the 8006-N minimum specification level, and there was no clear statistical ranking for the mixtures based on stability that could be compared with rankings provided by other mixture tests performed in this study. The same conclusion was found for the Marshall flows.

Table 8. Marshall mixture properties.

Mixture Type	Binder Type	Optimum Binder Content (%)	MSG	Stability (N)	Flow (0.25 mm)	Air Voids (%)	VMA (%)	VFA (%)
Properties of Plant-Produced Mixtures:								
Surface	AC-5	4.80	2.683	12 422	15.0	2.8	14.1	80.2
Surface	AC-10	4.80	2.691	13 046	15.8	2.7	13.8	80.4
Surface	AC-20	4.90	2.688	15 248	16.5	2.5	13.8	81.7
Surface	Novophalt	4.70	2.686	16 573	20.8	4.1	15.1	72.8
Surface	Styrelf	4.90	2.684	19 794	16.4	3.4	14.7	76.9
Base	AC-5	4.00	2.746	13 678	13.5	2.5	11.6	78.4
Base	AC-20	4.10	2.755	16 442	13.3	3.4	12.2	72.1
Properties of Laboratory-Prepared Mixtures:								
Surface	AC-5	4.85	2.699	11 565	14.5	3.0	13.9	78.4
Surface	AC-10	4.85	2.707	12 047	14.6	3.6	14.1	74.5
Surface	AC-20	4.85	2.706	11 232	17.6	2.9	13.5	78.5
Surface	Novophalt	4.85	2.699	16 125	16.8	4.2	14.9	71.8
Surface	Styrelf	4.85	2.701	18 536	22.8	4.0	14.7	72.8
Base	AC-5	4.00	2.750	13 295	12.8	4.3	13.1	67.2
Base	AC-20	4.00	2.750	14 168	12.4	4.2	13.0	67.7

Compaction Temperatures:

AC-5 = 121 °C
AC-10 = 127 °C
AC-20 = 135 °C
Novophalt = 141 °C
Styrelf = 141 °C

Marshall Blows Per Side:

Surface = 75
Base = 112

MSG = Maximum Specific Gravity of the Mixture.
VMA = Voids in the Mineral Aggregate.
VFA = Voids Filled With Asphalt.

8. Moisture Sensitivity

a. Pre-Construction Tests

Moisture sensitivity of the mixtures was evaluated prior to construction in accordance with ASTM Test Method D 4867.[6] In this test, the indirect (splitting) tensile strengths of conditioned and unconditioned specimens are measured. A tensile strength ratio (TSR), defined as the conditioned strength divided by the unconditioned strength, is computed in terms of a percentage. All tests were performed at an air-void level of 7 ±1 percent. The specimens were compacted by a Marshall hammer and had a diameter of 101.6 mm and thickness of 63.5 mm. Short-term oven-aging was not used because it was not part of ASTM D 4867 at the time these tests were performed.

The conditioning procedure consisted of saturating the compacted specimens so that 55 to 80 percent of their air voids were filled with water, soaking the specimens in a water bath at 60 °C for 24 h, and testing them for tensile strength at 25 °C along with the unconditioned specimens. The ASTM D 4867 optional freeze-thaw cycle was not included because it was not used by VDOT or paving contractors doing VDOT work. Mixtures with and without 1-percent hydrated lime were tested.

All mixtures with hydrated lime passed the test based on a minimum TSR of 80 percent. The TSR's of mixtures without hydrated lime ranged from 0.74 to 0.80. Even though these TSR's indicated only a slight susceptibility to moisture damage, the 1-percent hydrated lime requirement was maintained. At the time of construction, VDOT specified a TSR of 0.75.[2]

b. Tests After Construction

Tests on the five surface mixtures were repeated after construction using the stockpiled materials. A diametral modulus test, which provides a diametral modulus ratio (M_dR), was included in the evaluation along with a visual estimate of stripping. ASTM D 4867 was again used, except that the optional freezing cycle of -17.8 °C for 15 h was included to provide the most severe conditioning. The two base mixtures were not evaluated even though they were tested during the mixture design phase of the study. Theoretically, the BM-3 aggregate is too large for a specimen size of 101.6 by 63.5 mm.

The test results are shown in table 9. Pass/fail criteria of 80 percent for TSR, 70 percent for M_dR, and 10 percent for visual stripping have been recommended for conventional, dense-graded hot-mix asphalt.[5,12] Based on these criteria, the mixture with AC-5 (PG 58-34) failed the tests and the mixture with AC-10 (PG 58-28) was marginal. The other three mixtures passed the test, perhaps because they contained stiffer binders. Aggregate particles in the size range of 1.18 to 4.75 mm primarily stripped in the mixtures with the AC-5 and AC-10 (PG 58-34 and 58-28) binders, while aggregate particles greater than 12.5 mm stripped in the mixtures with the Novophalt and Styrelf binders. Visual stripping in the latter two mixtures was low. They were estimated to be 2 and 6 percent. No stripping was found in the pavements over the course of this study.

9. Superpave Volumetric Properties

Superpave was not used to design the mixtures because the methodology had not been finalized by the time of pavement construction. Mixtures produced from the stockpiled raw materials were compacted in the Troxler Model 4140 SGC after the Superpave test procedures and specifications were published in 1995.(3) The compaction temperatures were the same as those used in the Marshall mixture designs, which are shown in table 8.

All specimens were compacted to a single N-max of 174 revolutions. This N-max corresponded to an N-design of 109, which was specified by Superpave for a traffic level of 10 to 30 million ESAL's.(3) This N-design was chosen because it corresponded to a moderate to heavy level of traffic. However, it was not known how the number of ALF wheel passes at a controlled pavement temperature related to Superpave ESAL's.

Table 10 provides the optimum binder contents based on a 4.0-percent air-void level using four levels of N-design. The lower part of table 10 shows the air voids for the surface and base mixtures based on a 4.85- and 4.00-percent binder content, respectively. Both sets of data were taken from the same SGC compaction curves. The maximum specific gravity of the mixture and the bulk specific gravities of the specimens at N-max were used to determine the air voids in accordance with the 1995 Superpave specification.(3)

Superpave required a minimum VMA of 13.0 for a nominal maximum aggregate size of 19 mm, and 11.0 for a nominal maximum aggregate size of 37.5 mm. The data in table 10 show that the mixtures met these requirements at an N-design of 109. VFA was required to be between 65 and 75 percent for traffic levels equal to and greater than 3 million ESAL's. Table 10 shows that all seven mixtures had VFA above 75 percent. This upper limit is used to prevent rutting and bleeding. The Superpave requirements for VMA and VFA are based on a 4-percent air-void level. All mixtures at an N-design of 109 had air voids below 4.0 percent. These findings indicated that the gradations would have to be altered to meet the upper VFA criterion and, even with these alterations, the binder contents would probably have to be reduced. However, the VDOT mixtures used in this study did not have a history of rutting or bleeding, and the 75-blow SM-3 surface mixture had a tendency to ravel.

The low estimated N-designs at 4.0-percent air voids in table 10 indicated that the mixtures, according to Superpave, should only be used in low-volume pavements. This finding is not reasonable based on the field rutting performances of the two mixtures with AC-20 (PG 64-22) in Northern Virginia. Both mixtures are highly resistant to rutting when properly designed and constructed. Also, at the time of construction in 1993, VDOT generally used 4.5-percent binder by mass in BM-3 base mixtures, whereas only 4.0 percent was used in this study.

Table 9. Results from the ASTM D 4867 test method for moisture sensitivity performed on the five surface mixtures.

Pre-Superpave: Superpave PG:	AC-5 58-34	AC-10 58-28	AC-20 64-22	Novophalt 76-22	Styrelf 82-22
Average Indirect Tensile Strengths (TS) and Diametral Moduli (M_d) at 25 °C					
Wet TS, kPa	217	373	560	626	725
Dry TS, kPa	316	466	616	707	859
Wet M_d, MPa	455	960	1583	2526	1911
Dry M_d, MPa	713	1390	1571	3056	2445
Retained Ratios, Visual Stripping, Saturation, and Air Voids					
TS Retained Ratio, %	69	80	91	89	84
M_d Retained Ratio, %	64	69	101	83	78
Visual Stripping, %	17	10	0	2	6
Final Saturation, %	72	71	65	71	71
Air Voids, %	7.8	8.3	7.2	8.3	8.1

Table 10. Superpave Gyratory Compactor results.

Binder Type	Mixture Type	Binder Contents at 4-Percent Air Voids and Four Levels of N-design: 68	86	109	142
AC-5	Surface	4.85	4.50	4.25	4.00
AC-10	Surface	5.10	4.75	4.45	4.15
AC-20	Surface	5.10	4.80	4.50	4.25
Novophalt	Surface	5.00	4.50	4.15	3.95
Styrelf	Surface	4.55	4.20	3.95	3.80
AC-5	Base	3.90	3.65	3.50	3.35
AC-20	Base	3.90	3.65	3.45	3.25

Binder Type	Mixture Type	Air Voids at Binder Contents of 4.85 Percent for the Surface Mixtures and 4.00 Percent for the Base Mixtures, %: Marshall Impact Hammer	SGC N-design of 68	86	109	142	VMA, % at 109	VFA, % at 109	N-design, at 4.0 % Air Voids
AC-5	Surface	3.0	4.0	3.2	2.4	1.7	13.4	81.8	68
AC-10	Surface	3.6	4.6	3.8	3.1	2.3	13.6	77.9	82
AC-20	Surface	2.9	4.6	3.8	3.2	2.4	13.7	77.4	82
Novophalt	Surface	4.2	4.1	3.6	2.8	2.1	13.7	79.4	72
Styrelf	Surface	4.0	3.4	2.7	2.2	1.5	13.0	83.9	56
AC-5	Base	4.3	3.7	3.1	2.5	1.8	11.5	77.6	61
AC-20	Base	4.2	3.7	3.0	2.3	1.7	11.2	80.4	62

The Superpave volumetric requirements were based on relationships between mixture volumetric properties and the pavement performances of dense-graded mixtures. However, the majority of these mixtures were designed using the Marshall hammer and not a gyratory compactor. Adjustments to the N-designs given in the 1995 and 1998 Superpave specifications may be needed for some mixtures.[3] (Authors' note: AASHTO was reviewing new proposed N-designs when this report was being published in 1999.)

10. SGC Revolutions Needed to Obtain Air Voids That Matched the Final Air Voids of the Pavements

The air voids in and out of the wheelpaths were measured and evaluated during this study. The air-void data shown in table 11 were collected from 1994 to 1997. Analyses of the data are given in chapters 2 and 3. The information concerning the SGC is included in this chapter because it complements the preceding information on this compactor.

After each ALF pavement test was completed, the number of SGC revolutions needed to match the final air-void level of the pavement was determined. Table 11 shows the required number of revolutions based on the air voids in the top and bottom halves of the pavements. The average is also given.

The revolutions in table 11 can only be considered estimates for N-design, because the 1995 Superpave methodology for calculating the specimen air-void level as a function of SGC revolutions often led to air voids that were high at low revolutions relative to AASHTO T 166-93.[4] The air voids provided by the 1995 procedure included the air voids in contact with the cylindrical surface of the mold. These air voids would not be part of the specimen if the specimen were to be removed from the mold and tested using AASHTO T 166. AASHTO T 166, which is the standardized procedure for determining density, uses the saturated surface-dry condition to determine the volume of a specimen. This volume does not include the volume of any surface air voids. Therefore, AASHTO T 166 can provide a lower volume and a higher density compared with the SGC procedure. If this occurs, the revolutions provided by the SGC are too high. (Authors' note: This procedure was changed in 1999 so that the air voids would be directly measured using specimens removed from the molds at the desired N-design.) A second reason why the revolutions in table 11 can only be considered estimates is that it was assumed that the ultimate density of each pavement was reached before the pavement test was terminated. However, the change in pavement density was not monitored during the ALF tests, and the tests were not stopped at the same rut depth.

The data show that most of the gyratory revolutions were low relative to an N-design of 109. The revolutions ranged from 18 for the bottom half of the pavement with the Novophalt surface mixture tested at 58 °C to 128 for the bottom half of the pavement with the AC-5 (PG 59) base mixture tested at 58 °C. The revolutions were very low for the Novophalt and Styrelf mixtures, which generally had high air-void levels before and after testing. The data indicated that adjustments to the N-designs given in the 1995 and 1998 Superpave specifications may be needed for some mixtures.[3]

Table 11. Number of Superpave gyratory revolutions needed to obtain the final pavement air-void levels.

Superpave PG:	58-34	58-28	58-34	58-28	64-22
Conventional:	AC-5	AC-10	AC-5	AC-10	AC-20
Lane Number:	03	05	09	05	06
Final Rut Depth[1]	20	21	24	21	21
Test Temp, °C:	46	46	52	52	52
Top 100 mm of Pavement					
Initial Air Voids, %	7.4	6.4	5.6	8.3	8.6
Densification, %	3.6	2.0	1.8	1.5	3.1
Final Air Voids, %	3.8	4.4	3.8	6.8	5.5
Revolutions	71	70	71	36	53
Bottom 100 mm of Pavement					
Initial Air Voids, %	7.8	5.9	5.0	8.1	8.1
Densification, %	2.6	2.1	2.2	4.9	3.5
Final Air Voids, %	5.2	3.8	2.8	3.2	4.6
Revolutions	48	84	96	102	69
Entire Pavement					
Initial Air Voids, %	7.6	6.1	5.3	8.2	8.4
Densification, %	3.1	2.0	2.0	3.2	3.3
Final Air Voids, %	4.5	4.1	3.3	5.0	5.1
Revolutions	59	76	82	58	59
Applied ALF Wheel Passes (ESAL's)	250,000	125,000	3,500	25,000	215,000

[1]In the 200-mm thick asphalt pavement layer.

Table 11. Number of Superpave gyratory revolutions needed to obtain the final pavement air-void levels (continued).

	Surface Mixture					Base Mixture	
Superpave PG:	58-34	58-28	64-22	76-22	82-22	58-34	64-22
Conventional:	AC-5	AC-10	AC-20	Novphlt[2]	Styrelf	AC-5	AC-20
Lane Number:	09	05	10	08	07	11	12
Final Rut Depth[1]	26	27	31	9	22	24	24
Test Temp, °C:	58	58	58	58	58	58	58
Top 100 mm of Pavement							
Initial Air Voids, %	7.8	8.5	9.1	11.9	11.9	6.7	7.4
Densification, %	4.4	2.9	5.4	3.4	4.3	3.6	2.4
Final Air Voids, %	3.4	5.6	3.7	8.5	7.6	3.1	5.0
Revolutions	80	50	90	21	28	90	41
Bottom 100 mm of Pavement							
Initial Air Voids, %	7.0	8.4	8.3	10.8	12.8	6.0	7.4
Densification, %	4.2	5.1	4.9	1.8	4.6	3.8	2.3
Final Air Voids, %	2.8	3.3	3.4	9.0	8.2	2.2	5.1
Revolutions	97	99	99	18	24	128	39
Entire Pavement							
Initial Air Voids, %	7.4	8.4	8.7	11.4	12.3	6.3	7.4
Densification, %	4.3	4.0	5.2	2.6	4.4	3.7	2.4
Final Air Voids, %	3.1	4.4	3.5	8.8	7.9	2.6	5.0
Revolutions	88	70	93	19	26	109	41
Applied ALF Wheel Passes (ESAL's)	2,000	4,000	10,000	208,805	200,000	20,000	200,000

[1]In the 200-mm thick asphalt pavement layer.
[2]Novophalt.

Table 11. Number of Superpave gyratory revolutions needed to obtain the final pavement air-void levels (continued).

Superpave PG: Conventional: Lane Number: Final Rut Depth[1]	64-22 AC-20 06 21	76-22 Novophalt 08 17	82-22 Styrelf 07 21	76-22 Novophalt 08 17	82-22 Styrelf 07 21
Test Temp, °C:	64	70	70	76	76
Top 100 mm of Pavement					
Initial Air Voids, %	8.4	11.0	12.3	9.1	10.4
Densification, %	2.9	3.2	5.5	2.3	5.7
Final Air Voids, %	5.5	7.8	6.8	6.8	4.7
Revolutions	53	25	27	32	47
Bottom 100 mm of Pavement					
Initial Air Voids, %	9.0	10.1	12.1	10.4	9.9
Densification, %	5.3	3.6	5.5	4.2	4.4
Final Air Voids, %	3.7	6.5	6.6	6.2	5.5
Revolutions	90	35	29	38	38
Entire Pavement					
Initial Air Voids, %	8.7	10.6	12.2	9.7	10.2
Densification, %	4.1	3.4	5.5	3.2	5.1
Final Air Voids, %	4.6	7.2	6.7	6.5	5.1
Revolutions	69	29	28	35	42
Applied ALF Wheel Passes (ESAL's)	8,000	125,000	125,000	700,000	225,000

[1]In the 200-mm thick asphalt pavement layer.

11. Confounding Factors in This Study

This section of the report lists factors that could have affected the results of this study or the interpretation of the data. Most studies on asphalt mixtures and pavements have variables that cannot be controlled and often confound the results that are obtained. Even so, the numerous variables that affect pavement performance were controlled in this study to a higher degree than studies using in-service pavements.

Aggregates with high qualities, in terms of angularity, gradation, and hardness, were chosen for this study based on the expectation that the modified binders would be used in pavements containing high-quality aggregates that are subjected to heavy traffic levels. To justify the higher costs associated with most modified binders, these binders must provide benefits that match or exceed their cost regardless of the quality of the aggregate. The VDOT SM-3 surface mixture with the AC-20 (PG 64-22) binder has been used in Northern Virginia highways subjected to heavy traffic levels. This mixture is highly resistant to rutting when properly designed and constructed, although at the time of construction in 1993, VDOT also used an AC-30 asphalt binder with the SM-3 gradation in some pavements to further increase its resistance to rutting. The maximum allowable thickness is 50 mm. The SM-3 surface mixture used in this study also met the requirements for a VDOT IM-1A intermediate mixture.[2] The maximum allowable thickness for this application is 75 mm. Based on the experiences of many highway agencies, some mixtures are more resistant to rutting when used in thin lifts compared with thick lifts because the maximum aggregate size is approached as the thickness of the lift is decreased. Maximum layer thicknesses have been developed over time based on a variety of pavement experiences. Thus, even though the SM-3 surface mixture with the AC-20 (PG 64-22) binder is highly resistant to rutting when properly designed and constructed, its performance using a thickness of 200 mm is not known.

Although some mixtures rut less if used in thin lifts compared with thick lifts, thin lifts placed on Portland cement concrete may rut more than thick lifts when rutting is calculated as a percentage of the thickness of the lift. Complexities related to layer thickness and the properties of underlying layers were not evaluated in this study.

The BM-3 base mixture with AC-20 (PG 64-22) is used in Northern Virginia highways subjected to heavy traffic levels. This mixture is highly resistant to rutting when properly designed and constructed. However, a BM-3 mixture is always overlaid with intermediate and surface courses, whereas the two base mixtures constructed for this study were not overlaid. Therefore, for an equal amount of loading, the stresses from the load should be higher in the ALF pavements compared with in-service pavements. Even so, it was expected that the base mixture in lane 12 with the AC-20 (PG 64-22) binder would be highly resistant to rutting.

Even though the pavements in this study were heated to control the test temperature (discussed in chapter 2 of this report), a precisely controlled environment was not obtainable because the FHWA pavement test facility is an outdoor facility. When the pavement test temperature during a rutting test deviated by more than 6 °C from the target temperature due to a cold rain, the pavement test was suspended until the target temperature could be reestablished. A value of 3 °C was used for the fatigue-cracking tests. The effect of stopping the ALF, if any, on the pavement performance data was unknown and could not be taken into account.

One objective of this study was to validate several predictive laboratory mixture tests using ALF. However, the conventional test temperatures and applied stresses used by most of the laboratory mixture tests did not match the temperatures and stresses in the ALF pavement tests. Test temperatures and stresses in many laboratory mixture tests, such as wheel-tracking tests, have been chosen based on empirical relationships between the test data and the performances of in-service pavements that are subjected to some range in traffic level, vehicle speed, and temperature. These empirical relationships include the effects of having boundaries in the laboratory test, such as steel holders or platens, that are not the same as for in-service pavements.

Other possible confounding factors were (1) differences in material and volumetric properties from pavement to pavement, including the fact that the SM-3 surface mixtures contained 8-percent natural sand, while the BM-3 base mixtures contained 5-percent natural sand, and (2) binder properties can have seasonal variations that are a function of whether the pavement temperature has been increasing or decreasing over a period of several months. Seasonal variations are not considered in most studies.